Fe_3O_4-$LiMo_3Se_3$ Nanoparticle Clusters as Superparamagnetic Nanocompasses

Frank E. Osterloh,*,† Hiroki Hiramatsu,† R. K. Dumas,‡ and Kai Liu*,‡

Department of Chemistry and Department of Physics, University of California, One Shields Avenue, Davis, California 95616

Received June 6, 2005. In Final Form: July 25, 2005

A scaleable chemical approach to functional nanoscale analogues of the magnetic compasses in magnetotactic bacteria is described. $LiMo_3Se_3$-Fe_3O_4 nanowire−nanoparticle composites were synthesized by a reaction of 3-iodopropionic acid treated $LiMo_3Se_3$ nanowire bundles with oleic acid-stabilized Fe_3O_4 nanoparticles of 2.8, 5.3, and 12.5 nm size in tetrahydrofuran. Transmission electron micrographs show that the composite consists of Fe_3O_4 nanoparticles attached to the surfaces of the 4−6 nm thick nanowire bundles. UV/vis spectra reveal absorptions from the nanowire (506 nm) and magnetite components (280−450 nm), and IR spectra show characteristic bands for the propionic acid linkers and for the residual oleic acid ligands on the magnetite particles. In the presence of excess oleic acid, the nanocomposites undergo rapid disassembly, suggesting that Fe_3O_4 nanoparticles are bonded to nanowires via carboxylate groups from the linkers. Ultrasonication of a dispersion of the composite in THF produces individual $LiMo_3Se_3$-Fe_3O_4 clusters, which are 340 ± 107 nm long and 20 ± 5 nm thick, depending on the sonication time and Fe_3O_4 nanoparticle size. Field cooled and zero-field cooled magnetization measurements reveal that the blocking temperature (T_B = 100 K) of the clusters with 5.3 nm Fe_3O_4 is increased as compared to the free nanoparticles (T_B = 30 K). Directional dipolar interactions in the clusters lead to magnetic anisotropy, which makes it possible to align the clusters in a magnetic field (900 Oe).

Introduction

One of the challenges in nanoscience is to develop methods to remotely control the motion and orientation of nano- and microscale structures in real time.[1,2] An elegant way to achieve this goal is by the application of a magnetic field. It is well-known that materials with a magnetic anisotropy $\Delta\chi = \chi_{||} - \chi_{\perp}$ (here $\chi_{||}$ and $\chi_{\perp}$ are the susceptibilities along two perpendicular directions) will align their easy axis with the field lines of an external magnetic field.[3,4] By changing the orientation of the field or by changing the magnetic field gradient, it is then possible to orient and manipulate small structures in 3-D. Magnetically guided nano- and microstructures could potentially be used to stir reaction mixtures in closed microscale systems,[5] to drive microscale motors,[6] to operate microactuators and valves,[7,8] or to transport drugs and spectroscopic probes into organisms.[9−11] The feasibility of magnetically propelled microstir bars,[12] of magnetically guided catalytic nanomotors,[13] or of magnetically controllable micromirrors has been demonstrated.[14,15] Apart from generating forces, microscale anisotropic magnetic structures can also be used as magnetic sensors to detect the direction of magnetic field lines (compasses). One of the smallest known compasses occurs naturally in magnetotactic bacteria, which were discovered in 1975 by Blakemore.[16] The bacteria contain up to ∼45 magnetite (Fe_3O_4) nanoparticles of 40−120 nm diameter that form 1−3 μm long strings (see Figure 1).[17] Some bacteria contain greigite (Fe_3S_4) nanoparticles in the form of three to five separate chains.[18] Magnetic interactions among the adjacent magnetite particles couple them together to produce an easy axis along the chain, with a collective magnetic moment of about 10^{-13} emu.[19,20] The easy axis and magnetic moment enable the bacteria to align itself

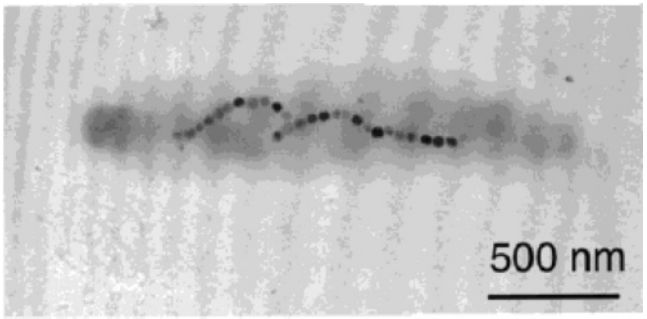

Figure 1. Transmission electron micrograph of a magnetotactic bacterium. Reproduced with permission from Albert P. Philipse.[22]

* Corresponding author. E-mail: fosterloh@ucdavis.edu.
† Department of Chemistry.
‡ Department of Physics.

(1) Feynman, R. P. *Eng. Sci.* **1960**, *33* (February).
(2) Craighead, H. G. *Science* **2000**, *290* (5496), 1532−1535.
(3) Lemaire, B. J.; Davidson, P.; Ferre, J.; Jamet, J. P.; Panine, P.; Dozov, I.; Jolivet, J. P. *Phys. Rev. Lett.* **2002**, *8812* (12), 5507.
(4) Bellomo, E. G.; Davidson, P.; Imperor-Clerc, M.; Deming, T. J. *J. Am. Chem. Soc.* **2004**, *126* (29), 9101−9105.
(5) Martin, J. I.; Nogues, J.; Liu, K.; Vicent, J. L.; Schuller, I. K. *J. Magn. Magn. Mater.* **2003**, *256* (1−3), 449−501.
(6) Zahn, M. *J. Nanopart. Res.* **2001**, *3* (1), 73−78.
(7) Deisingh, A. K. *Analyst* **2003**, *128* (1), 9−11.
(8) Pasquale, M. *Sens. Actuators, A* **2003**, *106* (1−3), 142−148.
(9) Freitas, R. A. *Nanomedicine*; Landes Bioscience: Austin, TX, 1999; p v.
(10) Requicha, A. A. G. *Proc. IEEE* **2003**, *91* (11), 1922−1933.
(11) Pankhurst, Q. A.; Connolly, J.; Jones, S. K.; Dobson, J. *J. Phys. D* **2003**, *36* (13), R167−R181.
(12) Bentley, A. K.; Trethewey, J. S.; Ellis, A. B.; Crone, W. C. *Nano Lett.* **2004**, *4* (3), 487−490.
(13) Kline, T. R.; Paxton, W. F.; Mallouk, T. E.; Sen, A. *Angew. Chem., Int. Ed. Engl.* **2005**, *44* (5), 744−746.
(14) Kim, J. Y.; Osterloh, F. E.; Hiramatsu, H.; Dumas, R. K.; Liu, K. *J. Phys. Chem. B* **2005**, in press.
(15) Osterloh, F. E. *J. Am. Chem. Soc.* **2002**, *124* (22), 6248−6249.
(16) Blakemore, R. *Science* **1975**, *190* (4212), 377−379.
(17) Bauerlein, E. *Angew. Chem., Int. Ed. Engl.* **2003**, *42* (6), 614−641.
(18) Hanzlik, M.; Winklhofer, M.; Petersen, N. *J. Magn. Magn. Mater.* **2002**, *248* (2), 258−267.

10.1021/la051498r CCC: $30.25
Published on Web 09/07/2005

and coordinate its motion with the geomagnetic field (0.5 Oe).[16,21,22]

In this paper, we describe a scalable chemical approach to functional nanoscale analogues of the magnetosomes of magnetotactic bacteria. The compasses were assembled by attaching Fe_3O_4 nanoparticles[23,24] as the magnetic component to 1-D $LiMo_3Se_3$ nanowires,[25,26] as structural templates. The synthetic structures are 20 ± 5 nm thick and 340 ± 107 nm long, and they can be aligned with a magnetic field at room temperature despite the lack of a permanent magnetic moment. In this paper, we report the synthesis of these nanoscale compasses and their structure, bonding, and magnetic properties.

Experimental Procedures

All operations were performed in a nitrogen atmosphere using degassed solvents. Tetrahydrofuran (THF) was dried over sodium/benzophenone. Oleic acid-coated Fe_3O_4 particles of variable size were synthesized by following the procedure described by Sun et al.[23] $LiMo_3Se_3$ was synthesized as described by Tarascon et al.[25,26] Centrifugations were performed in a Fisher Marathon 21 000 centrifuge (13 500 rpm = 21 000*g*). Disk-shaped FeNdB permanent magnets (∅1.27 cm × 0.25 cm) were obtained from Fisher Scientific.

Synthesis of $LiMo_3Se_3{\cdot}(CH_2)_2CO_2H$-$Fe_3O_4$ (1). A solution of 48 mg of 3-iodopropionic acid in 3 mL of water was added to a dispersion of 42 mg of $LiMo_3Se_3$ in 40 mL of water, and the mixture was heated to 80 °C in a water bath until the dispersion formed a gel (after approximately 4 h). The gel was then shaken up, and the deep red solution was heated again until the gel reformed. This procedure was repeated twice, after which 50 mL of ethanol was added to induce precipitation of the product. The solid was washed 3 times with a total of 90 mL of ethanol and then dispersed in 10 mL of THF. To form the composite, 1.0 mg of the modified nanowires was added as a wet solid to solutions of 5.0 mg of Fe_3O_4·OA (2.8, 5.3, or 12.5 nm) in 4 mL of THF and 1 mL of methanol. The mixtures were sonicated for 60 min and centrifuged at 13 750 rpm for the sample with the 2.8 and 5.3 nm magnetite and at 3600 rpm for the 12.5 nm magnetite. Alternatively, the products can be isolated by magnetic decantation. The colored supernatant was discarded, and the collected solids were then washed three more times with fresh THF until the supernatant stayed colorless and then were stored as wet solids under nitrogen.

Synthesis of $LiMo_3Se_3{\cdot}(CH_2)_2CO_2H$-$Fe_3O_4$ Clusters (2). Clusters were obtained by immersing a closed vial of a dispersion of 5 mg of **1** (with 2.8, 5.3, and 12.5 nm Fe_3O_4) in 10 mL of THF in an ultrasonication cleaning bath for 6 h. The deeply red−brown dispersions were centrifuged for 10 min at 20 000 rpm, and the black solid was collected by decanting off the supernatant and redispersed in 10 mL of THF with brief sonication. The resulting dispersions were kept for further experiments. Magnetically aligned clusters were obtained by depositing two to three drops of a freshly ultrasonicated THF dispersion of the clusters onto an unmodified Si wafer (5 × 5 mm) that had been placed between two circular FeNdB magnets at a distance of 1.25 cm and by drying in nitrogen for 30 s. The magnetic field strength at the center of the Si wafer was measured as 900 Oe.

Physical Measurements. Magnetic measurements were carried out with a Quantum Design Superconducting Quantum Interference Device (SQUID) magnetometer at a magnetic field strength of 100 Oe. Magnetic materials were placed into the magnetometer as films on a planar 5.0 × 5.5 mm^2 Si wafer (clusters) or as a solid solution in dried rubber cement (oleic acid coated Fe_3O_4 particles). Samples for scanning electron microscopy (SEM, FEI XL30-SFEG) were prepared by drop-coating the dispersion of the respective nanoparticle composites onto 25 mm^2 pieces of a Si wafer or onto aluminum stubs. Atomic force microscopy (AFM) scans were performed with a Digital Instruments Multimode AFM with a noncontact Si probe (150 kHz, 5 Nm) on samples deposited on Si wafers. For transmission electron microscopy (TEM, Philips CM12), samples were prepared by drop-coating the sample solutions onto holey carbon copper grids (Ted Pella). UV−vis spectra were recorded in standard quartz cuvettes using a Hewlett-Packard 8450A UV−vis spectrometer. The high-resolution TEM image was obtained on a Philips CM200 FEG microscope operated at 200 kV.

Results and Discussion

The reaction of $LiMo_3Se_3$ nanowire bundles with 3-iodopropionic acid and, subsequently, with oleic acid-stabilized Fe_3O_4 nanoparticles (2.8 ± 1.0, 5.3 ± 1.0, or 12.5 ± 2.4 nm) in THF produces the nanoparticle−nanowire composites (**1**) (see Figure 2).

The reaction relies on 3-iodopropionic acid as a covalent linker between nanoparticles and nanowires. The reagent is believed to react with the selenide portion of $LiMo_3Se_3$ with the displacement of iodide and formation of a Se−C bond. The CO_2H group then becomes available for binding to the Fe_3O_4 particles. A HRTEM image of the product suggests that the reaction is confined to $LiMo_3Se_3$ nanowires on the outside of the bundles. On this basis, the propionic acid-modified nanowires will be referred to as $LiMo_3Se_3{\cdot}(CH_2)_2CO_2H$.

Figure 3A−C shows TEM micrographs of **1** with 5.3 and 12.5 nm Fe_3O_4 nanoparticles. It can be seen that while the composite with 5.3 nm magnetite remains quite well-dispersed, the material with 12.5 nm magnetite forms aggregates that are probably supported by van der Waals and magnetic interactions among the larger particles. When the Fe_3O_4 nanoparticle size increases further, these nonselective interactions prevent the formation of a composite altogether. For example, when 31 ± 5 nm Fe_3O_4 particles were used in the reaction, globular nanoparticle aggregates (Figure S1) formed rather than the desired nanowire−nanoparticle composite.

The $LiMo_3Se_3{\cdot}(CH_2)_2CO_2H$-$Fe_3O_4$ (5.3 nm) nanocomposite contains ~84% of the magnetite particles directly bonded to the nanowire bundles. Interestingly, most of the particles are bonded to the sides of the nanowire bundles, and there are hardly any magnetite nanoparticles on top or underneath the bundles. This indicates that the nanowire−nanoparticle bonding is weak.

A HRTEM image of the composite is shown in Figure 3C. In contrast to raw exfoliated $LiMo_3Se_3$ nanowires,[27] the propionic acid-modified nanowires show lattice fringes only near the center of the bundles. This suggests that the reaction with the alkylating agent acid reduces the crystallinity of the bundles and does not affect $LiMo_3Se_3$ strands in the bundle center. The Fe_3O_4 nanoparticles, on the other hand, appear unchanged.

The infrared spectra of **1** (Figure S2) contain strong bands in the C−H stretching region (at 2960−2860 cm^{-1}), which indicate that **1** contains residual oleic acid surfactants on the surface of the Fe_3O_4 nanoparticles. These bands are also present in the IR spectrum of the pure

(19) Proksch, R. B.; Schaffer, T. E.; Moskowitz, B. M.; Dahlberg, E. D.; Bazylinski, D. A.; Frankel, R. B. *Appl. Phys. Lett.* **1995**, *66* (19), 2582−2584.
(20) Penninga, I.; Dewaard, H.; Moskowitz, B. M.; Bazylinski, D. A.; Frankel, R. B. *J. Magn. Magn. Mater.* **1995**, *149* (3), 279−286.
(21) Lee, H.; Purdon, A. M.; Chu, V.; Westervelt, R. M. *Nano Lett.* **2004**, *4* (5), 995−998.
(22) Philipse, A. P.; Maas, D. *Langmuir* **2002**, *18* (25), 9977−9984.
(23) Sun, S. H.; Zeng, H. *J. Am. Chem. Soc.* **2002**, *124* (28), 8204−8205.
(24) Liu, K.; Zhao, L.; Klavins, P.; Osterloh, F. E.; Hiramatsu, H. *J. Appl. Phys.* **2003**, *93*, 7951−7953.
(25) Tarascon, J. M.; DiSalvo, F. J.; Chen, C. H.; Carroll, P. J.; Walsh, M.; Rupp, L. *J. Solid State Chem.* **1984**, *58*, 290−300.
(26) Tarascon, J. M.; Hull, G. W.; DiSalvo, F. J. *Mater. Res. Bull.* **1984**, *19*, 915−924.
(27) Qi, X. B.; Osterloh, F. E. *J. Am. Chem. Soc.* **2005**, *127* (21), 7666−7667.

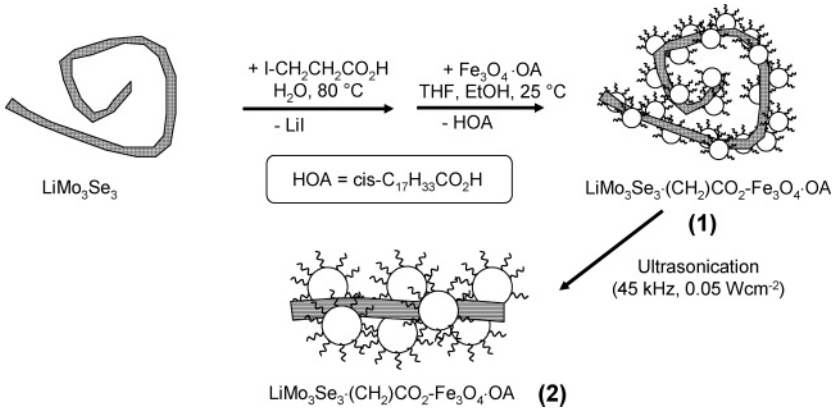

Figure 2. Chemical linkage of $LiMo_3Se_3$ nanowire bundles with Fe_3O_4 nanoparticles to form nanocomposites (**1**) and fragmentation into clusters (**2**).

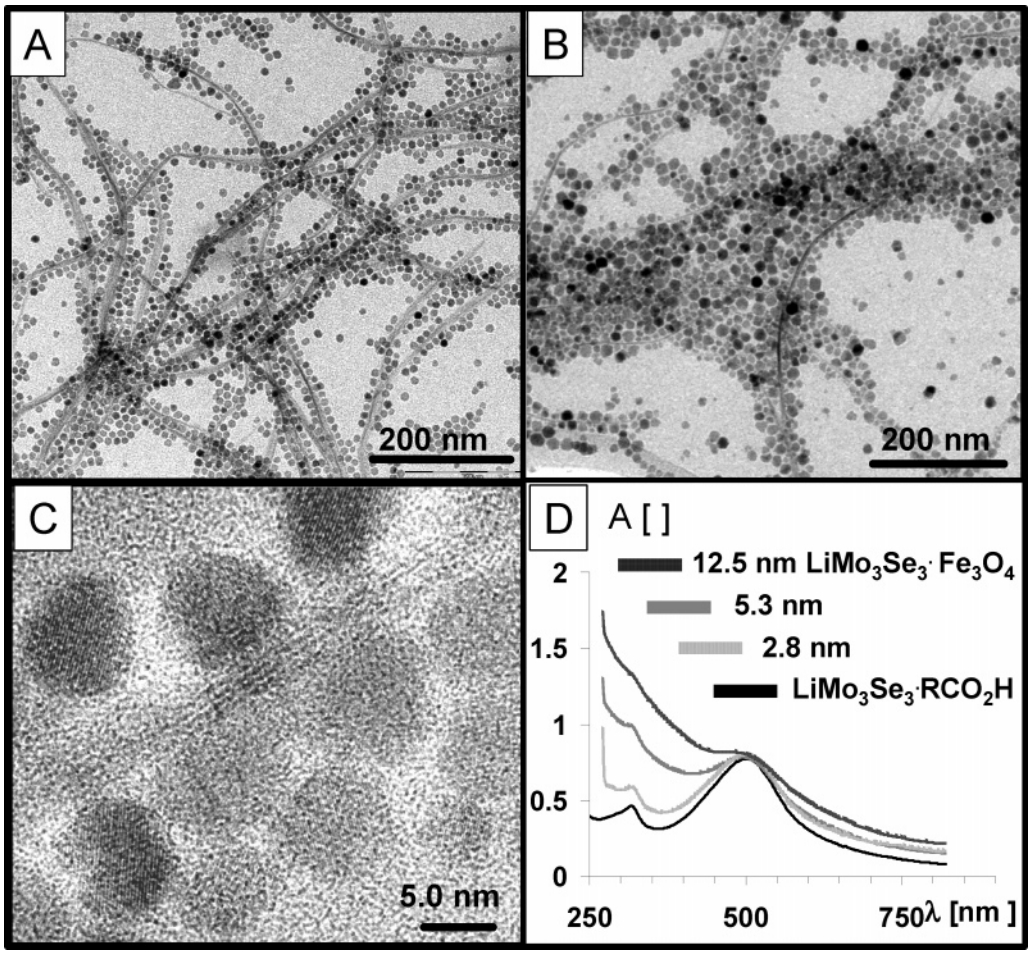

Figure 3. TEM images of nanowire−magnetite composites (**1**) (A) with 5.3 nm and (B) with 12.5 nm Fe_3O_4. (C) HRTEM of composite **1** with 5.3 nm Fe_3O_4 nanoparticles. (D) UV−vis spectra of **1** and of 3-iodo-propionic acid treated $LiMo_3Se_3$ nanowires (all in THF).

OA-supported Fe_3O_4 nanoparticles. In addition, the spectrum of **1** contains a contribution from the iodopropionic acid groups, which can be discerned in the spectrum for the modified nanowires (at 2930/2860 cm^{-1}). That spectrum also shows a weak peak at 1741 cm^{-1} that can be assigned to the carbonyl C−O stretch of propionic acid. A peak at 1641 cm^{-1} is likely from associated water (O−H bend).

The reaction of **1** with millimolar concentrations of oleic acid followed by brief ultrasonication leads to rapid disassembly of the nanocomposite (see Figure S3). The fact that the $LiMo_3Se_3$·$(CH_2)_2CO_2H$-Fe_3O_4 interaction can be broken by carboxylic acid suggests that the composite is stabilized by covalent Fe−O bonds between ferric/ferrous ions of the Fe_3O_4 cores and CO_2^- groups of the propionic acid.

The optical properties (Figure 3D) of **1** are characterized by a strong absorption of $LiMo_3Se_3$·$(CH_2)_2CO_2H$ at 500 nm, which is attributed to a Mo−Se LMCT process. In addition, samples of **1** have an absorbance tail that reaches from the ultraviolet into the visible region of the spectrum. This broad band is associated with the band gap absorption of Fe_3O_4, and its extinction depends on the content and size of the Fe_3O_4 nanoparticles.

Ultrasonication of a dispersion of the nanoparticle−nanowire composite **1** in THF using a standard benchtop

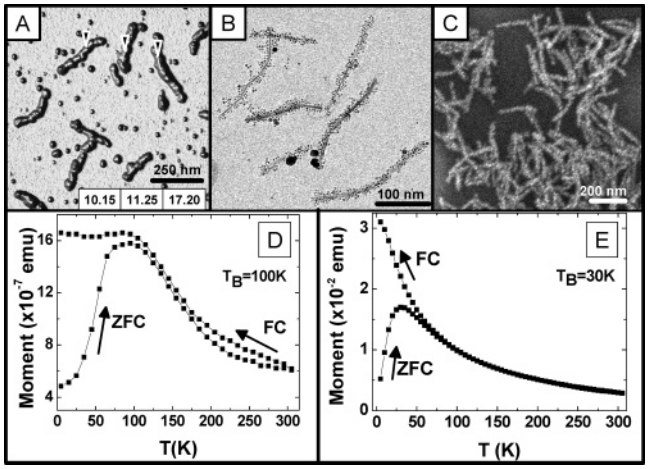

Figure 4. AFM (A), TEM (B), and SEM (C) images of clusters **2** containing 2.8 nm Fe_3O_4. Measured heights of the clusters (nm) are shown in panel A. Temperature dependence of magnetization measured after zero-field cooling (ZFC) and field cooling (FC) for clusters **2** containing 5.3 nm Fe_3O_4 nanoparticles bonded onto $LiMo_3Se_3{\cdot}(CH_2)_2CO_2H$ (D) and for a frozen solution of 5.3 nm Fe_3O_4 nanoparticles (E).

ultrasonication cleaning bath with a calculated power output of 0.05−0.1 W cm^{-2} produces discrete nanoparticle clusters **2**. These clusters can be isolated magnetically or via centrifugation from the solution, and they can be redispersed in nonpolar solvents (e.g., THF) with brief ultrasonication. Atomic force micrographs and TEM/SEM images of **2** (Figure 4) show that the nanoparticle clusters are 340 ± 107 nm long fragments of the original composite. Most of these clusters have kinks that cannot be observed in the composite **1**. The kinks are caused by the forces that act on the nanowires during ultrasonication and represent the first stage of nanowire breakage. Cohen theoretically estimated the ideal tensile strength (the maximum sustainable force before breakage) of $LiMo_3Se_3$ nanowires to be on the order of 15.5 nN.[28] For a 4−6 nm thick bundle of seven to 37 nanowires, this value should increase by about 1 order of magnitude. Our experiments show that these values can be achieved with an ultrasonic cleaning bath with a power output of 0.1 W cm^{-2}. A side effect of ultrasonication is the dissociation of magnetite particles from the nanowires. This occurs more frequently for larger particles than for smaller ones, and it restricts synthetic access to clusters with Fe_3O_4 core sizes larger than 12.5 nm using ultrasonication. The greater mobility of the larger particles is probably related to their larger mass and, consequently, due to the larger forces that act on the clusters during ultrasonication.[29]

The temperature dependence of the magnetic properties of **2** (5.3 nm Fe_3O_4) was measured on a film of clusters mounted on a silicon wafer after zero-field cooling (ZFC) and field cooling (FC), as shown in Figure 4D. The data show that the clusters have a blocking temperature T_B of 100 K, above which they are superparamagnetic. This temperature is significantly higher than the 30 K blocking temperature of a dispersion of well-separated oleic acid-coated 5.3 nm Fe_3O_4 particles (Figure 4E). The difference between the two blocking temperatures indicates strong magnetic interactions between magnetic nanoparticles in **2**, which stabilize the magnetic moments of the Fe_3O_4 nanoparticles against thermal fluctuations. For two

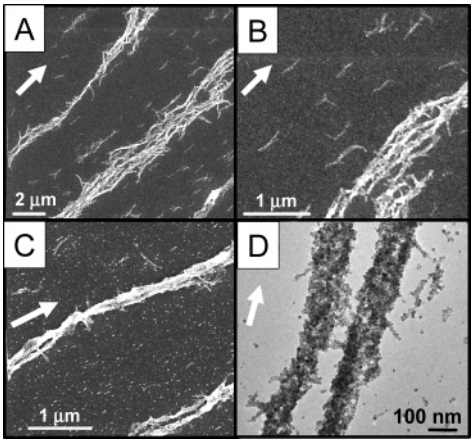

Figure 5. SEM (A−C) and TEM (D) micrographs of magnetically aligned $LiMo_3Se_3{\cdot}(CH_2)_2CO_2H$-$Fe_3O_4$ clusters (A and B) of **2** (2.8 nm Fe_3O_4) and (C and D) of **2** (5.3 nm Fe_3O_4).

coupled magnetic dipoles (4×10^{-17} emu for 5.3 nm Fe_3O_4) in a head-to-tail orientation at 7.0 nm center-to-center distance, the calculated magnetostatic energy is 5.6 meV.[30] The thermal energy kT required to break this interaction is reached at 67 K. This value is close to the observed blocking temperature of **2**.

Because of the approximately uniaxial distribution of the magnetic particles in the clusters (see Figure 4B), the sum of the magnetic dipole interactions is expected to be larger in the parallel than the perpendicular direction to the clusters. This produces a magnetic easy axis that aligns with the longer cluster axis, which mimics that in the magnetotactic bacteria. The expected magnetic anisotropy of the clusters can be confirmed experimentally by exposing the clusters to static magnetic fields. Figure 5 shows the arrangement of clusters obtained after drop-coating a dispersion of clusters in THF under the influence of a 900 Oe magnetic field oriented parallel to the plane of the substrate (direction shown as arrow). It can be seen that over the course of 30 s (the evaporation time of the solvent), all the clusters align with the magnetic field direction. Deviations from the magnetic direction occur for bent clusters (due to kinks in the nanowire backbone) and for clusters that are part of larger aggregates. Furthermore, most of the clusters containing 2.8 nm Fe_3O_4 and virtually all of those containing 5.3 nm Fe_3O_4 particles form columnar aggregates along the magnetic field direction. The columns, which are a result of dipolar interactions between magnetically aligned clusters, are typically observed when dispersions of superpara- and ferromagnetic particles (ferrofluids) are exposed to magnetic fields.[31,32] $LiMo_3Se_3$ nanowires without attached Fe_3O_4 nanoparticles do not align in a magnetic field, which shows that the magnetic anisotropy of the clusters **2** arises from dipolar magnetic interactions among the Fe_3O_4 particles.

Conclusion

Our study demonstrates that pseudo-uniaxial superparamagnetic nanostructures can be chemically assembled from magnetite nanoparticles (2.8−12.5 nm) and $LiMo_3Se_3{\cdot}(CH_2)_2CO_2H$ nanowire building blocks. The chemical assembly route is limited to particle sizes smaller

(28) Ribeiro, F. J.; Roundy, D. J.; Cohen, M. L. *Phys. Rev. B* **2002**, *65* (15), -.
(29) Prozorov, T.; Prozorov, R.; Suslick, K. S. *J. Am. Chem. Soc.* **2004**, *126* (43), 13890−13891.
(30) Chikazumi, S. *Physics of Ferromagnetism*, 2nd ed.; Oxford Science Publications: Oxford, 1997; p 7.
(31) Martin, J. E.; Venturini, E.; Odinek, J.; Anderson, R. A. *Phys. Rev. E* **2000**, *61* (3), 2818−2830.
(32) Pileni, M. P. *Adv. Funct. Mater.* **2001**, *11* (5), 323−336.

than ~14 nm because for larger Fe_3O_4 particles magnetic and van der Waals aggregation tends to dominate the reaction preventing the formation of a well-defined product. In the $LiMo_3Se_3{\cdot}(CH_2)_2CO_2H$-$Fe_3O_4$ clusters, dipolar interactions among the Fe_3O_4 particles produce a magnetic anisotropy that allows magnetic alignment with a magnetic field (~900 Oe). In this function, the clusters resemble the compasses of magnetotactic bacteria. However, because the synthetic structures are about 5−10 times smaller, fields much stronger than the geomagnetic field (0.5 Oe at sea level) are required for alignment. In contrast to the ferromagnetic magnetosomes in the bacteria, the synthetic structures do not possess a permanent magnetic dipole at room temperature and therefore cannot distinguish between magnetic north and south.

Acknowledgment. This work was supported by the Petroleum Research Fund (38057-G5 and 39153-G5B), by the National Science Foundation (CTS-0427418), and by the University of California−Davis (startup and CLE funds). We thank Prof. Susan Kauzlarich for providing a furnace for the synthesis of starting materials, Dr. William Casey in the Department of Land Air and Water Resources at UC Davis for providing the AFM (purchased with NSF-EAR94-14103), and the staff and facilities of the National Center for Electron Microscopy for support.

Supporting Information Available: Scanning electron micrographs and IR spectra of $LiMo_3Se_3{\cdot}(CH_2)_2CO_2H$-$Fe_3O_4$. This material is available free of charge via the Internet at http://pubs.acs.org.

LA051498R